A solar furnace for copper smelting in Chile: assessment of economic benefits and reductions in greenhouse gas emissions

Dimitrij Chudinzow[1, a)], Dirk Switon[1] and Ludger Eltrop[1]

[1] Institute of Energy Economics and Rational Energy Use (IER), University of Stuttgart, Heßbrühlstraße 49a, 70565 Stuttgart, Germany

[a)] Corresponding author: dimitrij.chudinzow@ier.uni-stuttgart.de

Abstract

This work investigates the integration of a solar furnace (SF) into the smelting processes of copper in a flash furnace under Chilean solar irradiation conditions. A computer model of a 1 MW_{th} solar furnace, inspired by the French solar furnace in Odeillo, with a total heliostat specular area of 2,835 m² was developed and the annual energy contribution of the SF for copper smelting in a flash furnace was simulated. Economic benefits through fossil fuel savings in three different flash furnaces were compared with the investment costs for a SF for a lifetime of 50 years. Furthermore, reductions in greenhouse gas emissions ($CO_{2\text{-eq}}$-emissions) through fuel saving were calculated. The results show that, depending on the fuel type used in the flash furnace, up to 24% in $CO_{2\text{-eq}}$-emissions and up to 10% of lifetime costs can be saved.

Keywords: Solar Furnace, Chile, Smelting, Copper, Greenhouse Gas Emissions

1. Introduction

Metal smelting requires huge amounts of thermal energy. Usually, this energy demand is covered by liquid fossil fuels or electricity. While the utilization of solar energy for electricity generation and medium temperature thermal applications is widespread, yet there is no commercial use of solar energy for high temperature applications like metal smelting.

Solar furnaces (SF), like the French solar furnace in Odeillo (Fig. 1), collect and reflect direct solar radiation

Fig. 1: French solar furnace in Odeillo (World's Largest Solar Furnace n.d.)

with 63 heliostats onto a parabolic shape (concentrator) which in turn is redirected into a receiver. In the focal point temperatures up to 3,800 °C can be reached (Trombe, Le Vinh 1973). Currently, solar furnaces are used in research institutions only, e.g. for high temperature calcium carbide (CaC_2) formation (Paizullakhanov, Faiziev 2006), for smelting (Abdurakhmanov et al. 2008a) or material testing (Neumann 2005), (PROMES b).

Chile's economically most important produced metal is copper, which contributed 88% to Chilean export shipment values from the mining sector in 2015 (Servicio Nacional de Geología y Minería 2016). The fossil fuel consumption for copper production amounted 21.9 TWh in 2014, of which 7% were needed for smelting (Fundación Chile n.d.). The use of solar energy for metal smelting might have the potential to reduce costs and

Selection and/or peer review under responsibility of Scientific Committee
doi:10.18086/swc.2017.26.03 Available at http://proceedings.ises.org

greenhouse gas emissions through replacing fossil fuels. Therefore, this work investigates the technical and financial potential of the integration of solar furnaces into high temperature smelting of copper under Chilean conditions as well as possible reductions in $CO_{2\text{-eq}}$-emissions.

2. Previous Work

Funken et al., from the German Aerospace Center DLR, developed a mini-scale SF powered rotary kiln for smelting 1 kg of aluminum scrap (Funken et al. 2001). They report a duration for smelting in the range of 0.5 to 6 h, depending on irradiance conditions (Cologne, Germany) and the achieved temperature. Additionally, a large scale solar kiln (capacity: 8 t) was designed and the heliostat field was optimized. The benefit of the applied solar smelting was the reduced amount of resulting flue gas that had to be cleaned. Furthermore, cost savings due to avoided fuel consumption can be expected. This concept is further investigated in the SOLAM project, a German-South African research initiative (DLR 2015). Abdurakhmanov et al. investigated different types of smelting furnaces using the large solar furnace in Uzbekistan (Abdurakhmanov et al. 2008b).

3. Integration of a solar furnace into copper smelting

3.1 Weather data

The solar resource website *Explorador Solar* provides both typical meteorological years (TMY) data files in an hourly resolution and weather measurement datasets in a 10-minute resolution (Ministerio de Energía 2017). To achieve a higher accuracy, a TMY was developed based on the weather measurement datasets from *Crucero 2*, which is located 45 km from Chuquicamata, the world's largest open-pit copper mine (latitude: -22.1647°, longitude: -69.339777°). For the selection of representative months, the direct normal irradiation (DNI) was used as the only criterion, since this is the most influencing parameter on the performance of a SF. The DNI values from the developed TMY are shown in Fig. 2. Clearly this location exhibits exceptional high solar irradiation.

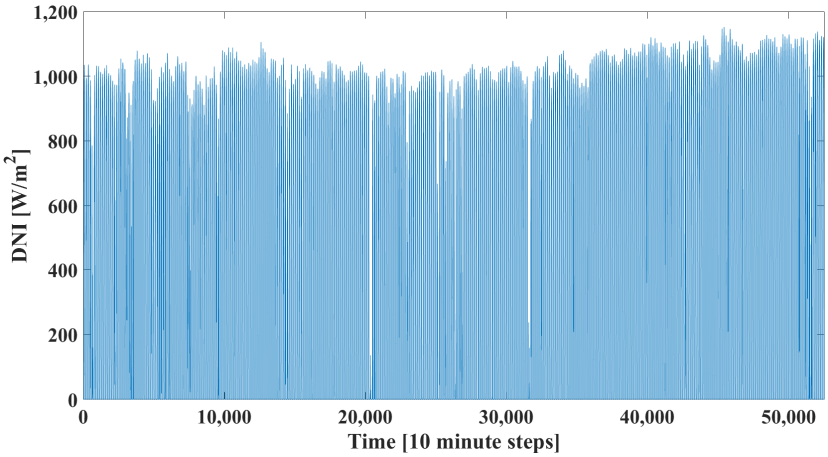

Fig. 2: DNI values from developed TMY based on *Crucero 2* measurements

3.2 Development of a solar furnace model in Matlab

Fig. 3 shows the subcomponents of the developed SF model. The layout of the heliostat field and the design of the concentrator is based on the French SF in Odeillo (PROMES a). The formulas to compute the time-variant cosine loss factor and the time-dependent orientation of each heliostat are taken from (Stine, Geyer 2001). The resulting total thermal power output of the SF system is calculated according to eq. (1).

$$P_{SF} = A_{Heliostat} \cdot DNI(t) \cdot \eta_{rh} \cdot \eta_{rc} \cdot \eta_{sbh} \cdot \eta_{sbc} \cdot \eta_{int} \cdot \eta_{aa} \cdot \eta_{circ} \sum^{n_{Heliostats}} \eta_{cos,i}(t) \qquad \text{eq. (1)}$$

The cosine loss factors were calculated for each heliostat separately to achieve more accurate results. The values from the other efficiencies are given in Appendix I.

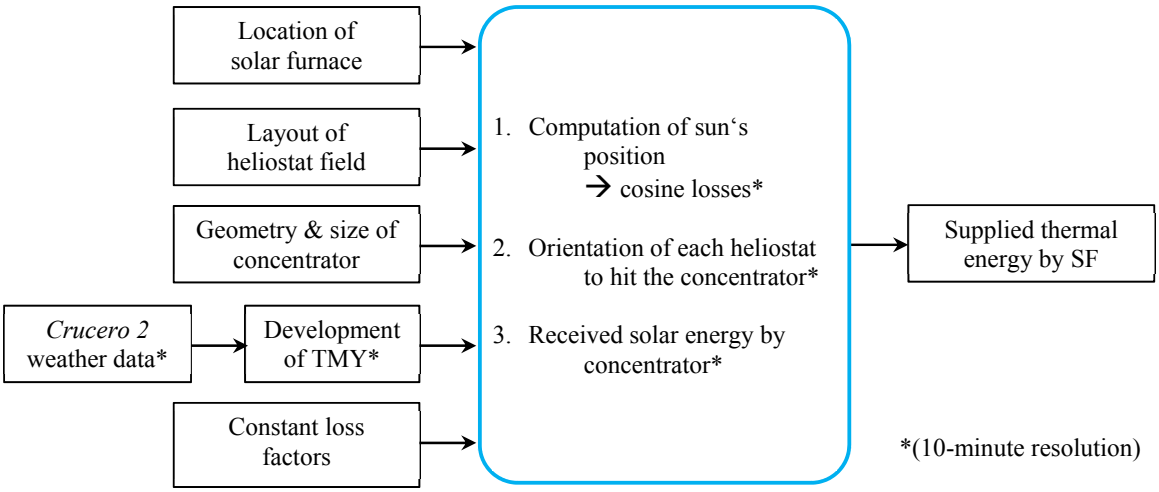

Fig. 3: Subcomponents of developed SF model

Fig. 4 shows a plot of the modelled SF in Chile.

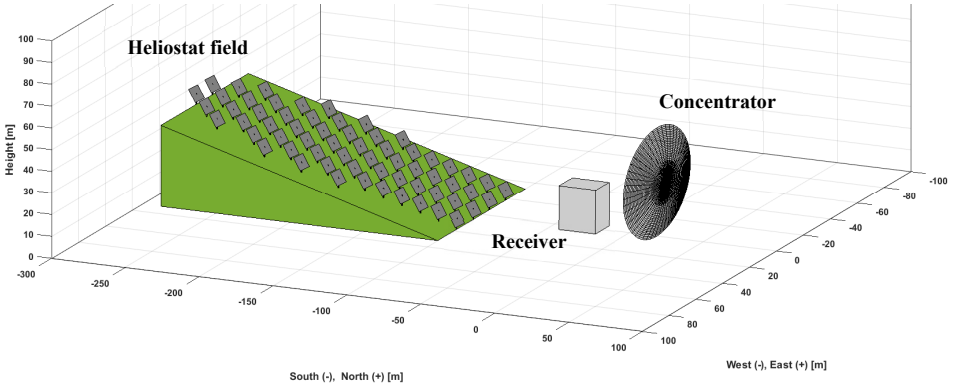

Fig. 4: Plot of the modelled SF and heliostat field located in Chile

In Fig. 5 the simulated thermal output of the SF is shown. We can clearly observe that most of the time the output of the SF exceeds the design point of 1 MW_{th}, due to high DNI irradiation found in northern Chile. It is

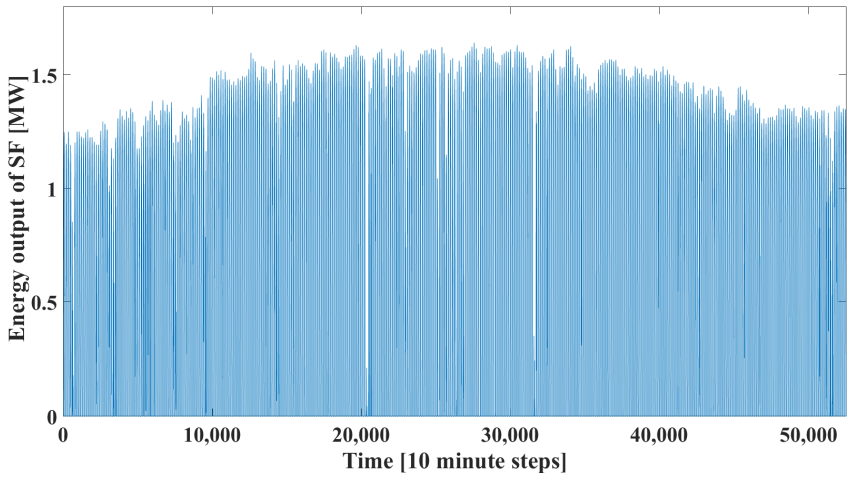

Fig. 5: Thermal output of the modelled SF, located in Chile

interesting to observe, that in winter time on the southern hemisphere the performance of the SF is higher than in summer. This can be explained by two factors: first, the DNI in northern Chile is constantly high throughout the whole year; secondly, the field performance of a point-focusing heliostat field is better in winter time when the sun hangs low in the sky.

3.3 Integration into copper smelting

The basic concept for the implementation of a SF into the copper smelting process is shown in Fig. 6. In this work we investigate three different flash furnaces, which need additional fuel for maintaining the thermal equilibrium. The thermal energy delivered by the SF contributes to the thermal equilibrium in a flash furnace and thus allows savings in fossil fuel consumption.

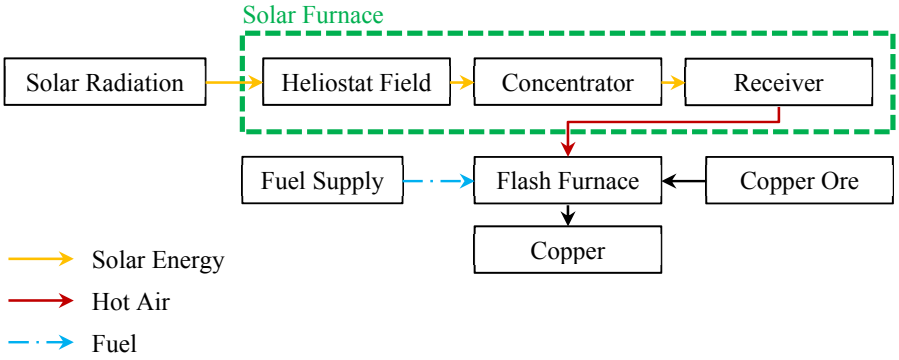

Fig. 6: Basic concept of the implementation of a solar furnace (SF) into the copper smelting process in a flash furnace

The properties of the investigated three flash furnaces are shown in Tab. 1, based on (Schlesinger 2011).

Tab. 1: Data of three flash furnaces used for cost analysis, based on (Schlesinger 2011)

	Flash furnace 1	**Flash furnace 2**	**Flash furnace 3**
Start of operation	1983	1972	1971
Concentrate feed [t/d]	2,000 (23-29% Cu)	2,241 (29.2% Cu)	3,830 (28.8% Cu)
Matte production [t/d]	1080 (54-56% Cu)	1129 (63.3% Cu)	1895 (64% Cu)
Fuel consumption [kg/h]	198.2 (Bunker C)	1,200 (Coal)	147 (Coal) + 404 (Diesel)
Fuel costs [USD$_{2017}$/h]	69	54	350
$\dot{m}_{Fuel}$·LHV [MW]	2.18	9.6	6.27

Since the fuel type varies among different flash furnaces, we took all three different fuels into account. Tab. 2 contains the characteristics of the fuel types.

Tab. 2: Lower heating values (LHV), specific $CO_{2\text{-eq}}$-emissions and costs of considered fuel types (Fürkus n.d.; Emission factors in kg CO2-eq per unit)

Fuel	**LHV [kWh/kg]**	**Specific $CO_{2\text{-eq}}$-emissions [kg$CO_{2\text{-eq}}$/kWh]**	**Costs [USD$_{2017}$/kg]**
Hard Coal	7.80	0.32	0.045
Diesel	11.83	0.3	0.85
Bunker C	11.00	0.29	0.35

3.4 Costs of the solar furnace

To estimate the costs of a SF, we adapted the specific costs for a heliostat from (new energy update 2017) and updated the figure to USD$_{2017}$, using an average inflation rate of 2%/a. This leads to specific heliostat costs of 147.9 USD$_{2017}$/m². Furthermore, we assume that heliostat costs constitute a share of 40% of total costs of a thermal CSP system (i.e. excluding “balance of plant”, “thermal energy storage” and “power block” from the cost components of a CSP power tower), based on the cost breakdown from (IRENA 2012). Finally, we assume annual operation and maintenance ($O\&M_{annual}$) costs as 5% of the initial investment. For the SF in Chile, a

heliostat field consisting of 63 heliostats (45 m² each) was designed (cf. Appendix II). With this information we calculate:

$$I_0 = \frac{147.89 \frac{USD_{2017}}{m^2} \cdot 63\ Heliostats \cdot \frac{45m^2}{Heliostat}}{40\%} = 1{,}048{,}170\ USD_{2017} \qquad \text{eq. (2)}$$

$$O\&M_{annual} = I_0 \cdot 5\% = 52{,}409\ USD_{2017} \qquad \text{eq. (3)}$$

Due to the fact that the French SF was completed in 1970 and is still in operation, a lifetime of T=50 years is assumed (Trombe, Le Vinh 1973). Taking into account an interest rate of *i*=2.5% (Chile Interest Rate 2017), we determine the present value PV_{SF} of the solar furnace as follows:

$$PV_{SF} = I_0 + O\&M_{annual} \cdot \frac{(1+i)^T - 1}{i \cdot (1+i)^T} = 2{,}534{,}597\ USD_{2017}$$

4. Results

The developed SF model calculated an annual thermal energy output of 4.66 GWh/a for the location in Northern Chile. To determine monetary savings, we assume that this energy output reduces the fossil fuel consumption of the flash furnaces each year. This gives us the net present values of the fuel costs of the three flash furnaces (FF1, FF2, FF3) without and with the integration of a SF for a lifetime of 50 a, as shown in Fig. 7. We can observe, that under the described assumptions, the integration of a SF is profitable for FF1 (-10%) and FF3 (-8%). Since in FF2 cheap coal is used, the integration of a SF is not profitable (+13%). "SF Costs" is the net present value of the SF, taking into account the investment costs I_0 and the annual O&M costs over the course of 50 a.

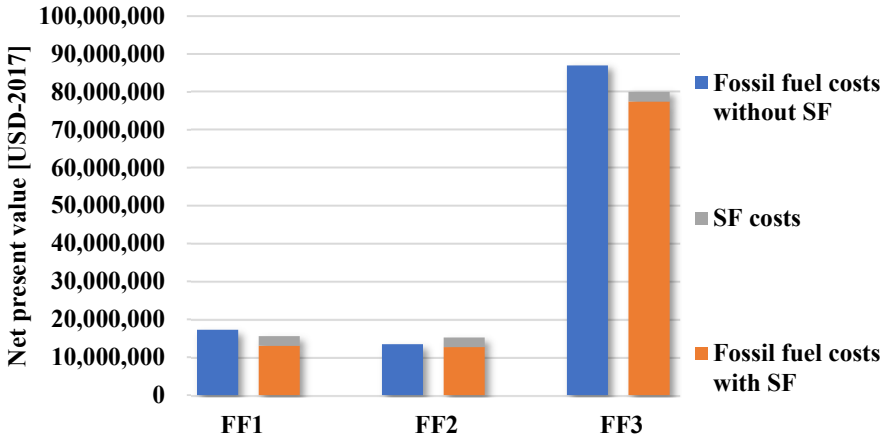

Fig. 7: Net present values of fuel costs for three flash furnaces, without and with the integration of a solar furnace

In Fig. 8 reductions in $CO_{2\text{-eq}}$-emissions through the integration of a SF are depicted. We can clearly see that the integration of a SF can reduce $CO_{2\text{-eq}}$-emissions. For FF1, FF2 and FF3 the savings are 24.4%, 5.6% and 8.9%, respectively.

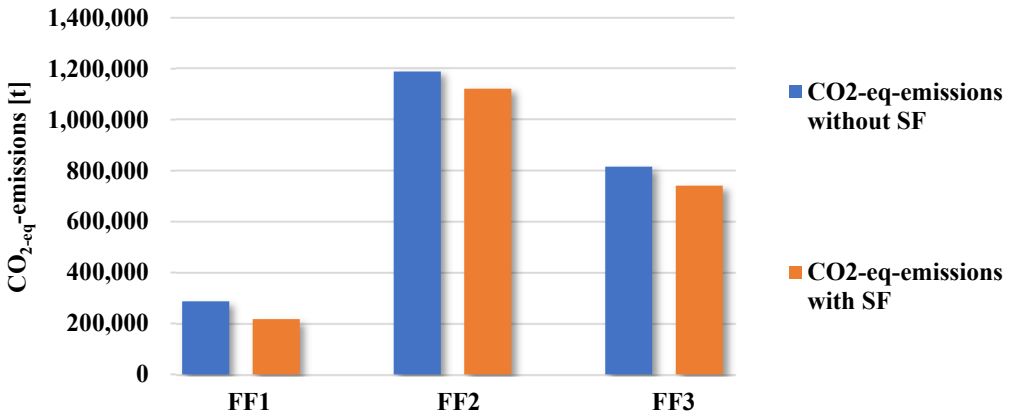

Fig. 8: $CO_{2\text{-eq}}$-emissions for three flash furnaces, without and with the integration of a solar furnace, after 50 a

5. Conclusion and outlook

In this work, we investigated the economic benefits as well as reductions in $CO_{2\text{-eq}}$-emissions through the integration of a solar furnace (SF) into copper smelting in Chile. A solar furnace was modelled in Matlab and the annual thermal energy production in the North of Chile was simulated. A SF with the same design as the French SF in Odeillo, located in Chile, would generate around 4.66 GWh/a. Depending on the type of fuel that is used in a flash furnace, up to 10% of fossil fuel costs and 24% in $CO_{2\text{-eq}}$-emissions could be saved. The results show, that it can be advantageous in economic and environmental terms to put more efforts in the research on solar aided metallurgy. Future research should focus on the concrete development of a solar aided flash furnace, taking into account specific metallurgical requirements during the smelting process.

6. Appendix

Appendix I – Values of efficiencies used in the developed SF model

References: (Stine, Geyer 2001; Téllez et al. 2014; Ewert, Fuentes n.d.; Segal 2012; The Circumsolar Radiation 2013):

η_{rh}:	Reflectivity of the heliostats, including the contamination with dust and the aging	= 0.94
η_{rc}:	Reflectivity of the concentrator, the same values as for the heliostats were selected	= 0.94
η_{sbh}:	Shading and blocking factor for the heliostat field	= 0.98
η_{sbc}:	Shading and blocking factor for the concentrator	= 0.98
η_{int}:	Factor for the interception of the solar rays	= 0.97
η_{aa}:	Atmospheric attenuation of the solar rays in the solar furnace system	= 0.97
η_{circ}:	Factor for the circumsolar radiation	= 0.8
$\eta_{cos,i}(t)$:	Cosine loss factor of each heliostat	Calculated in 10-minute steps

Appendix II – Parameters of the French solar furnace in Odeillo

Position	Concentrator	Heliostats	Heliostat field
Latitude: 42.2939° Longitude: 2.0145°	40 m height, 54 m width, focal length= 18 m	N=63, 7.5 m height, 6 m width	8 terraces, 16 heliostat rows in total

Reference (Centre National De La Recherche Scientifique (CNRS) n.d.)

7. Publication bibliography

Abdurakhmanov, A. A.; Akbarov, P. Yu.; Akhadov, Zh. Z.; Mamatkosimov, M. A.; Sobirov, Yu. B.; Turaeva, U. F. (2008a): Creating melting furnaces based on the large solar furnace. In *Appl. Sol. Energy* 44 (4), pp. 284–287. DOI: 10.3103/S0003701X08040129.

Abdurakhmanov, A. A.; Akbarov, R. Yu.; Sobirov, Yu. B. (2008b): Analysis of operating characteristics of various smelting furnaces on a Large Solar Furnace. In *Applied Solar Energy* 44 (1), pp. 24–27. DOI: 10.3103/S0003701X08010088.

Centre National De La Recherche Scientifique (CNRS) (n.d.): High Temperature Solar Energy. Odeillo. Available online at https://www.gtri.gatech.edu/history/files/media/other-publications/High_Temp_Solar_Energy_Pamphlet.pdf, checked on 7/19/2017.

Chile Interest Rate (2017). Available online at https://tradingeconomics.com/chile/interest-rate, checked on 9/1/2017.

DLR (2015): SOLAM - solar aluminium smelting in a directly irradiated rotary kiln. Available online at http://www.dlr.de/sf/en/desktopdefault.aspx/tabid-9315/16078_read-46207/, checked on 3/16/2017.

Emission factors in kg CO2-eq per unit. Available online at http://www.winnipeg.ca/finance/findata/matmgt/documents/2012/682-2012/682-2012_Appendix_H-WSTP_South_End_Plant_Process_Selection_Report/Appendix%207.pdf, checked on 10/10/2017.

Ewert, M.; Fuentes, Navarro (n.d.): Modelling and simulation of a solar tower power plant. RWTH Aachen University. Available online at http://www.mathcces.rwth-aachen.de/_media/5people/frank/solartower.pdf, checked on 9/14/2017.

Fundación Chile (n.d.): From copper to innovation. Mining technology roadmap 2035. Available online at http://programaaltaley.cl/archivo-publicaciones/hoja-de-ruta-tecnologica-para-la-mineria-en-ingles/, checked on 10/11/2017.

Funken, Karl-Heinz; Roeb, Martin; Schwarzboezl, Peter; Warnecke, Heiko (2001): Aluminum Remelting using Directly Solar-Heated Rotary Kilns. In *J. Sol. Energy Eng* 123 (2), pp. 117–124. DOI: 10.1115/1.1355242.

Fürkus, S. (n.d.): Heizkostenrechner. Available online at http://heizkostenrechner.eu/heizwert-brennwert-tabelle.html, checked on 10/10/2017.

IRENA (2012): Concentrating Solar Power.

Ministerio de Energía (2017): Explorador Solar. Available online at http://www.minenergia.cl/exploradorsolar/, checked on 9/14/2017.

Neumann, Andreas (2005): Solar Furnace Ten Years Old. DLR. Available online at http://www.dlr.de/en/Portaldata/1/Resources/kommunikation/publikationen/109_nachrichten/dlr-nari109_en_76-79.pdf, checked on 3/9/2017.

new energy update (2017). CSP tower installation costs drop on heliostat innovations, pre-assembly. Available online at http://analysis.newenergyupdate.com/csp-today/csp-tower-installation-costs-drop-heliostat-innovations-pre-assembly, checked on 10/12/2017.

Paizullakhanov, M. S.; Faiziev, Sh. A. (2006): Calcium carbide synthesis using a solar furnace. In *Tech. Phys. Lett.* 32 (3), pp. 211–212. DOI: 10.1134/S1063785006030102.

PROMES a. The solar furnace of Odeillo font romeu. Available online at https://www.promes.cnrs.fr/index.php?page=the-solar-furnace-of-odeillo-font-romeu, checked on 10/11/2017.

PROMES b. Available online at https://www.sollab.eu/promes.html, checked on 3/9/2017.

Schlesinger, Mark E. (2011): Extractive metallurgy of copper. Amsterdam, Boston: Elsevier.

Segal, A. (2012): Optimum layout of heliostat field when the tower-top receiver is provided with secondary concentrators. Available online at http://sfera.sollab.eu/downloads/JRA/WP13/R13.3b_SFERA_WP13T2_Opt_HelioField_Secondary_TopReceiver.pdf, checked on 10/1/2017.

Servicio Nacional de Geología y Minería (2016): Anuario de la Minería de Chile 2015. Available online at http://www.sernageomin.cl/pdf/mineria/estadisticas/anuario/Anuario-de-la-Mineria2015.pdf, updated on 3/17/2017.

Stine, B. William; Geyer, Michael (2001): Power From The Sun. Available online at http://www.powerfromthesun.net/book.html, checked on 9/14/2017.

Téllez, F.; Villasante, C.; Burisch, M. (2014): State of the Art in Heliostats and Definition of Specifications. Survey for a low cost heliostat development. Available online at https://www.stage-ste.eu/deliverables/STAGE_STE_Deliverable_12_1.pdf, checked on 9/15/2017.

The Circumsolar Radiation (2013). Available online at http://www.black-photon.de/products/circumsolar-radiation/71-measurement-principle-csr-sensor.html, checked on 10/12/2017.

Trombe, Felix; Le Vinh, Albert Phat (1973): Thousand kW solar furnace, built by the National Center of Scientific Research, in Odeillo (France). In *Solar Energy* 15 (1), pp. 57–61. DOI: 10.1016/0038-092X(73)90006-6.

World's Largest Solar Furnace (n.d.). Available online at http://www.atlasobscura.com/places/worlds-largest-solar-furnace, checked on 10/5/2017.